

Understanding milling induced changes: Some results[†]

K CHATTOPADHYAY^{1,2}, N RAVISHANKAR², T A ABINANDANAN¹
and VIJI VARGHESE^{1*}

¹Department of Metallurgy, and ²Materials Research Centre, Indian Institute of Science, Bangalore 560 012, India
e-mail: kamanio@metalrg.iisc.ernet.in

Abstract. The effect of mechanical milling on materials has been studied using simple model systems. The results show that milling leads to enhancement in both thermodynamic driving force and transport kinetics. A study of some characteristic physical properties of the milled samples in comparison to the bulk shows how milling affects the properties.

Keywords. Mechanical milling; driven systems; mechanochemistry.

1. Introduction

Milling is identified as one of the robust processing routes for synthesizing a variety of materials. Commonly applied to the materials in solid state, the most noticeable change with milling is the reduction in the particle size, generally to nanoscale. In addition to size refinement, milling has received wide acceptability due to its potential to drive the changes at ambient conditions which are either not possible or require vigorous conditions in conventional processing routes.^{1–3} For example, while unfavourable decomposition steps restrict the high temperature chemical reactions of a number of materials, they can be easily brought about through milling at room temperature itself.⁴ Similarly, while the solubility of materials restricts the use of solution chemistry for synthesis, milling bypasses such limitations.^{5,6} The versatility and broad area of applicability of this technique are evident not only in chemical reactions, but also in changes such as phase transitions, alloying and amorphization.^{2,3} Thus, although the effect is known through antiquity,⁷ there has been a resurgence of interest in recent times.

Solutions to many of the processing problems encountered in mechanical alloying and mechanochemical reactions require basic understanding of the processes that take place with input of mechanical energy at rapid rates. These include the mechanism by which the changes take place, the influence of milling in deciding the direction and kinetics of the change, and the characteristics of the resultant product. In recent times, we have been carrying out an experiment-based programme of study using simple systems in order to understand the basic processes associated with the mechanical milling of solids.^{8–15} We show that milling leads to enhancement in the thermodynamic driving force as well as the transport kinetics. Also, we demonstrate the characteristic physical properties of the milled product in comparison to the bulk. A brief summary of the salient results obtained through this effort is presented in this article.

[†]Dedicated to Professor C N R Rao on his 70th birthday

*For correspondence

2. Thermodynamic driving force in milling induced changes

Thermodynamics plays a major role in the selection of phases. This is most striking if the phase is a new metastable phase not existing in the equilibrium phase diagram. A clear illustration of its importance is the effect of milling on Ag–Te system at room temperature.¹⁰ It is known that rapid solidification of Te rich alloys yields a simple cubic phase with an **a**Po structure.¹⁶ Te undergoes transformation at high pressure to both the **a**Po and the **b**Po structures for which data on change in modulus are available.¹⁷ Figure 1 shows the computed free energy curves of these two possible metastable phases together with the equilibrium phases and a possible amorphous phase. A straight line between the free energies of Ag and Te gives the free energy of the mechanical mixture. However, the contribution from an increased area of grain boundaries raises the free energy curve of nanosized (20 nm) elemental mixtures of Ag and Te phases significantly. As a result, a large driving force develops for the formation of the metastable **a**Po structure. The experimental X-ray diffraction patterns of the samples milled for different times in a planetary mill are shown in figure 2. The emergence of the simple cubic phase at the later stages of milling when the grain sizes reaches nanometric size is consistent with the thermodynamic prediction.

The actual physical mechanism for the grain size reduction differs for ductile and brittle materials.^{18,19} However, in all cases, the increase in the surface area leads to a

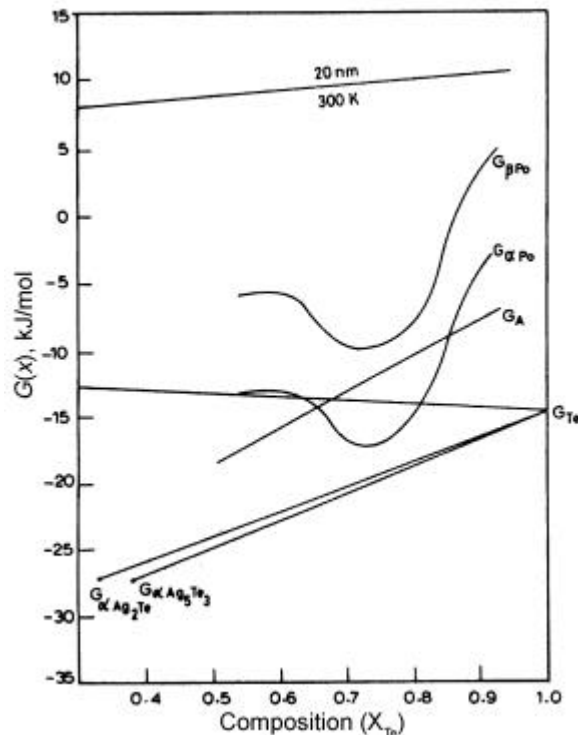


Figure 1. Free energy curves of the Ag–Te system at room temperature including the metastable phases.

dynamics (CD) model, based on Martin's model for driven systems,²¹ along with an effective potential formalism was used to explain the phase stability under milling.¹² The competing dynamics model considers the process as a competition between mixing (through milling) and demixing (thermal). The difference in the phase stability calculated under irradiation or mechanical alloying from that of the thermal equilibrium bulk stability leads to the modification of the phase diagram for driven alloys. We tried to extend this formalism with a reasonable estimate of the ballistic diffusivity and modified effective potential during the process.¹² The phase diagram thus obtained is critically compared against the reported experimental results. The model in short can be described as follows.

The effective potential Φ is,

$$\Phi = G + K, \quad (1)$$

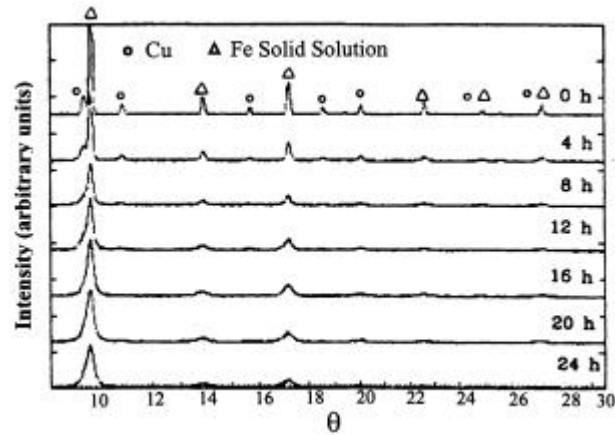


Figure 3. X-ray diffraction patterns of mechanically alloyed Fe-20%Cu powders milled at room temperature for different times.

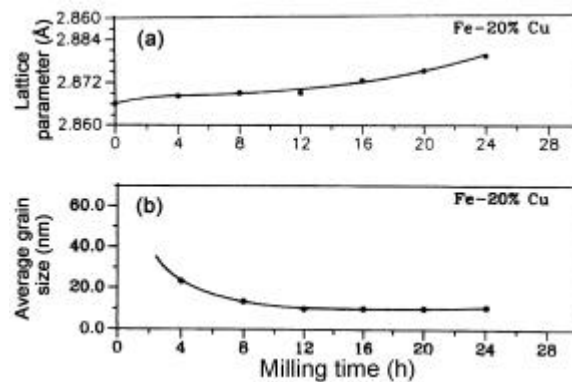


Figure 4. Plots showing changes in (a) lattice parameter, (b) grain size as a function of the milling time.

where, G is the Gibbs free energy and K is ballistic potential

$$K \quad \frac{dK}{dx} = D^b/M = \frac{x D_A^b + (1-x) D_B^b}{x(1-x)[x M_A + (1-x) M_B]}, \quad (2)$$

where D^b is the ballistic diffusivity and M is the mobility.

If K_A and K_B are the partial molar ballistic potentials, then,

$$K = (1-x)K_A + xK_B, \quad (3)$$

and the Gibbs–Duhem equation would be

$$x dK_B + (1-x) dK_A = 0, \quad (4)$$

if we assume $D_A^b = D_B^b = D^b$ and the integration constants as zero, then the overall potential could be expressed as,

$$\Phi = G + \frac{(1-x) D^b}{M_A} \ln \frac{(1-x)}{x M_A + (1-x) M_B} + \frac{x D^b}{M_B} \ln \frac{x}{x M_A + (1-x) M_B}. \quad (5)$$

The dynamical phase diagram obtained for the binary system Ag–Cu using the CD model with a calculated ballistic diffusivity ($10^{-22} \text{ m}^2 \text{ s}^{-1}$) is given in figure 5. The striking feature of the phase diagram is the self closing miscibility gap at low temperature. Also it is seen that the low temperature miscibility increases with increasing ballistic diffusivity. Uneishi *et al*²² demonstrated complete solid solubility in mechanically milled Ag–Cu alloys at room temperature. Later Herr and Samwer²³ showed that samples milled at 383 and 423 K exist as a mixture of two phases even after prolonged milling. Thus the trend predicted by CD model is consistent with the experimental observation. Between the two competing factors, milling becomes the deciding parameter for the stability of phases when the contribution from demixing (thermal) becomes insignificant at low temperature compared to that from mixing (ballistic).

3. Kinetics in milling aided changes

In principle, the input of mechanical energy can affect the bonding within the system and thereby the kinetics of the process apart from the thermodynamic driving force. No

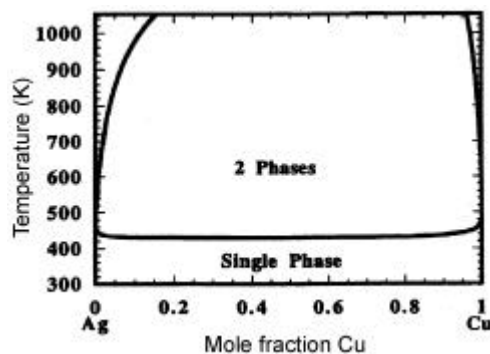


Figure 5. Dynamical phase diagram of Ag–Cu system.

systematic study on this aspect is available in the literature. In order to understand the factors influencing the kinetics in milling induced changes, the displacement of copper through different methods by different metals from copper sulphate in different forms have been selected as model reactions.¹³

In the solid state copper sulphate crystallizes with varying water of crystallization and $\text{CuSO}_4 \cdot 5\text{H}_2\text{O}$ is the most common of all. A physical mixture of Fe and $\text{CuSO}_4 \cdot 5\text{H}_2\text{O}$ does not promote the displacement of copper both at ambient and higher temperatures though the driving force does exist for the change. However, the reaction proceeded to certain extent at room temperature when a piece of Fe was immersed inside $\text{CuSO}_4 \cdot 5\text{H}_2\text{O}$ and compacted (figure 6). While the reaction possibly did not progress much into the bulk in compaction route, the displacement of Cu in $\text{CuSO}_4 \cdot 5\text{H}_2\text{O}$ and Fe mixture was complete within few hours when it is subjected to milling (figure 7). The size of reactant particles, proper mixing and intimate contact between reactants become quite important while the overall conversion in bulk is considered. Milling enhances both mixing and size reduction and provides intimate interface in each collision momentarily. Though, the amount of reaction mixture experiencing a single collision is small, the entire reaction mass would have undergone collision over a period of time due to the dynamic nature of the process yielding a bulk product.

Although the reduced diffusion length and dynamic nature of process end up in faster conversion in bulk, the factors contributing to faster reaction and diffusion also come into picture when the process is looked at microscopic level. Both milling and system characteristics play significant roles in deciding the rate of reaction as well as the mass transport. Over a period of milling it is reflected in the over all kinetics of the change.

The thermal analysis of milled $\text{CuSO}_4 \cdot 5\text{H}_2\text{O}$ showed significant deviation from as obtained sample including additional weight loss step suggesting weakening in the bonding. The weakening in the bond strength can lead to enhancement in reaction rate. Apart

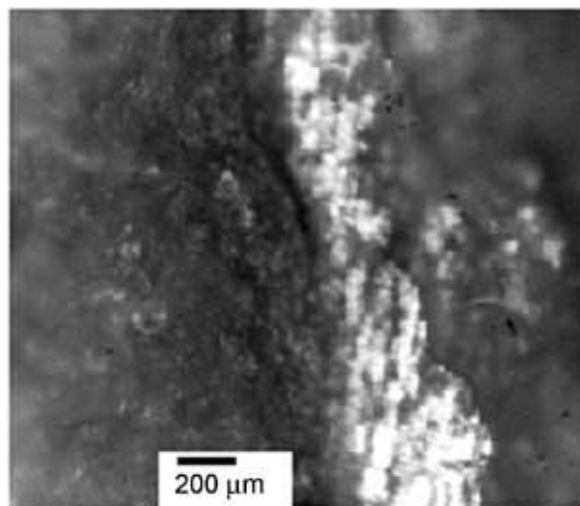


Figure 6. Optical micrograph of Fe- $\text{CuSO}_4 \cdot 5\text{H}_2\text{O}$ system, pressed at 150 MPa. A strip of Fe was kept between layers of $\text{CuSO}_4 \cdot 5\text{H}_2\text{O}$ tiny crystals and pressed. Cu deposition can be seen.

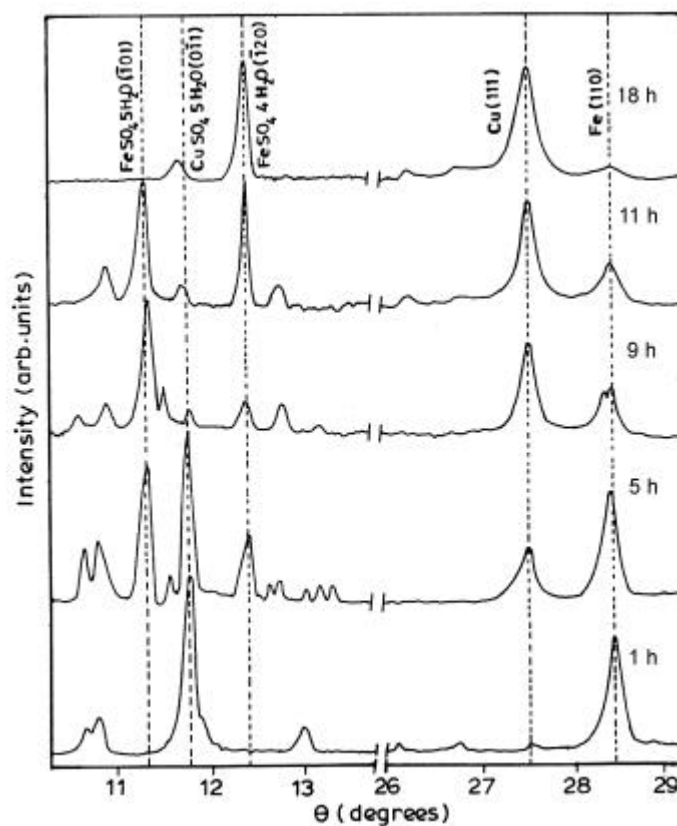


Figure 7. A series of X-ray diffraction patterns as a function of milling time showing the progress of mechanochemical reaction in the solid mixture of Fe and $\text{CuSO}_4 \cdot 5\text{H}_2\text{O}$. The most intense reflection of reactants, intermediate and products are marked.

from affecting bonds, milling also introduces all types of defects leading to substantial size reduction. The presence of high concentration of defects and increased surface area promotes reaction rate as well as diffusion. The presence of pressure gradient generated at the time of collision can also contribute to the process.

The extent to which these will influence the kinetics depends on the nature of the system as well. Figure 8 shows that while copper was liberated progressively with milling, the phase jurbanite, $(\text{Al}(\text{SO}_4)(\text{OH}) \cdot 5\text{H}_2\text{O})$ emerged as the end sulphate product in $\text{CuSO}_4 \cdot 5\text{H}_2\text{O}$ -Al system.¹⁴ Interestingly, the reaction was not faster compared to the reaction in $\text{CuSO}_4 \cdot 5\text{H}_2\text{O}$ -Fe though the driving force is much larger. Additionally, the absence of the expected end product $\text{Al}_2(\text{SO}_4)_3 \cdot x\text{H}_2\text{O}$ in any stage of the reaction clearly brings out the difficulty in simultaneous electron transfer from three copper ions to two aluminium ions along with simultaneous ion rearrangements within the crystal to form a completely different molecular structure for the product sulphate. Thus in $\text{CuSO}_4 \cdot 5\text{H}_2\text{O}$ -Al system the slow reaction rate lowered the rate of displacement of Cu.

The factors influencing the diffusion such as crystal structure and diffusivity of ions can also affect the kinetics. The reduction in water of hydration ($\text{CuSO}_4 \cdot \text{H}_2\text{O}$) reduced the

rate of displacement of Cu by Fe by several times though the driving force for the change was approximately the same as that in $\text{CuSO}_4 \cdot 5\text{H}_2\text{O}$ -Fe system. The open structure of $\text{CuSO}_4 \cdot 5\text{H}_2\text{O}$ with channels aids faster diffusion.²⁴ In contrast, the tightly packed three-dimensional network of chemical bonds in the structure of $\text{CuSO}_4 \cdot \text{H}_2\text{O}$ ²⁵ implies a difficulty in the transport of Cu and Fe. Even when the driving force for the displacement of copper is considerably lesser, the higher diffusivity of the metal like Sn through the crystal has resulted in extremely faster reaction rate in $\text{CuSO}_4 \cdot 5\text{H}_2\text{O}$ -Sn system (figure 9). Thus, apart from the effect of milling, the characteristics of the system also contribute significantly to the kinetics of milling induced changes.

4. Physical properties of milled products

4.1 Magnetic properties of Finemet alloys

The Fe-Cu-Nb-Si-B alloys (Finemet) are known for their attractive soft magnetic properties. The dispersion of nanocrystalline $\alpha\text{-Fe}(\text{Si})$ phase in a residual amorphous

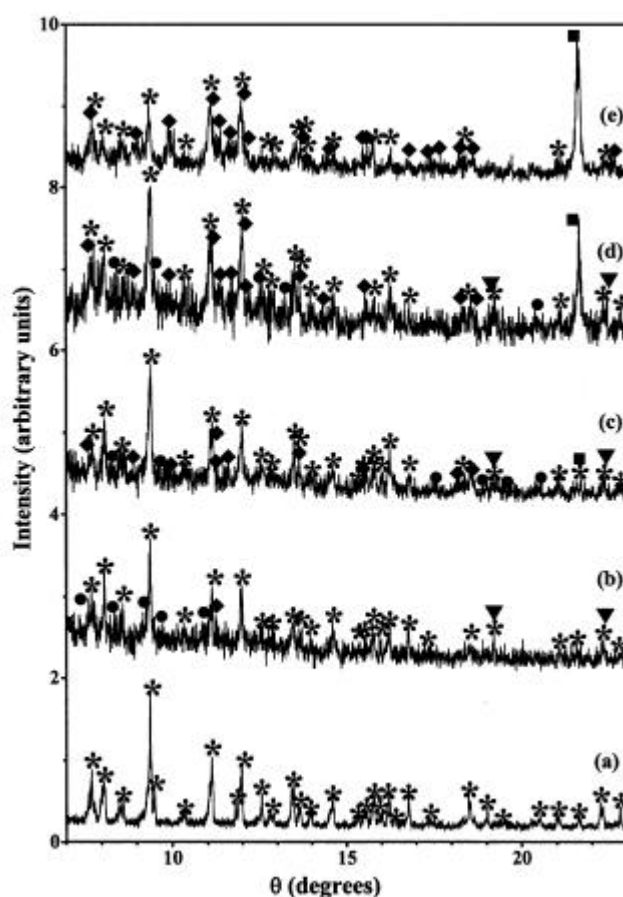


Figure 8. The X-ray diffraction patterns of (a) $\text{CuSO}_4 \cdot 5\text{H}_2\text{O}$ powder, (b) $\text{CuSO}_4 \cdot 5\text{H}_2\text{O}$ -Al system after 3 h, (c) 10 h, (d) 20 h and (e) 75 h, recorded using $\text{Cu}_{\text{K}\alpha 1}$. * $\text{CuSO}_4 \cdot 5\text{H}_2\text{O}$, \blacktriangledown Al, \bullet intermediate, \blacklozenge $\text{Al}(\text{OH})\text{SO}_4 \cdot 5\text{H}_2\text{O}$, and \blacksquare Cu.

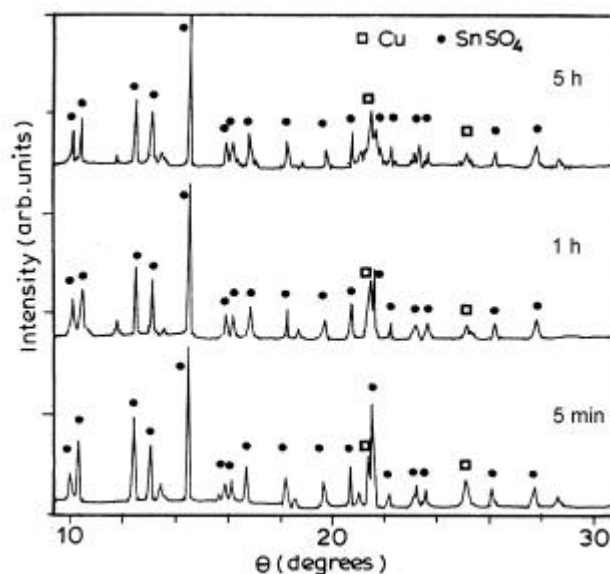


Figure 9. A series of X-ray diffraction patterns as a function of milling time in the solid mixture of Sn and $\text{CuSO}_4 \cdot 5\text{H}_2\text{O}$. Reaction is complete within five minutes.

matrix reduces the effective magnetic anisotropy and magnetostriction in the Finemet alloys. Thus, the soft magnetic property of the alloy arises from its characteristic microstructure. The microstructural dependence of the magnetic properties was explained by random anisotropy model (RAM) proposed for amorphous ferromagnets by Alben *et al.*²⁶

Minor addition of Cu to the conventional Fe–Si–B acts as nucleating agent while minor addition of Nb inhibits the grain growth of FeSi phase that crystallizes from the amorphous phase during annealing. The Fe–Si–B alloy loses its soft magnetic properties when it is completely crystallized while a controlled precipitation of the nanocrystalline state from the amorphous phase improves the property. The Finemet alloy with a desirable microstructure can be prepared by the melt-spinning technique followed by the annealing at elevated temperatures. We have analysed the role of magnetic interactions between the nanocrystalline and the residual amorphous phase by comparing the alloy produced by both melt spinning and mechanical alloying.⁸

Typical X-ray diffraction patterns of alloys produced by mechanical alloying (milled for 60 h), melt spinning as well as annealed melt spun ribbon are given in figure 10. The analysis clearly shows that the melt spun ribbons are completely amorphous while, only the nanocrystalline $\alpha\text{Fe}(\text{Si})$ phase is formed from the elemental powders during ball milling. The melt-spun alloy after heat treatment at 550°C for 1 h has both nanocrystalline phase and residual amorphous phase.

Figure 11 shows the thermomagnetic curves of mechanically alloyed and melt-spun Finemet alloys. From these curves, one can conclude that the magnetization of the melt-spun amorphous ribbon is more stable against temperature than mechanically alloyed sample. The magnetization of melt-spun ribbon abruptly decreases to zero at 354°C, which is the Curie temperature of the as quenched ribbon. The ribbon changes from

ferromagnetic to paramagnetic state at 354°C and it remains paramagnetic up to 500°C. The magnetization abruptly increases at 510°C followed by a decrease towards zero at 590°C. The increase corresponds to the crystallization of the α -FeSi phase from the amorphous matrix, which is also supported by the microstructural studies of the melt-spun ribbons using TEM. The transition at 590°C is the Curie temperature of α -FeSi.

The coercivity of mechanically alloyed samples are two orders of magnitude larger than that of the annealed melt spun ribbon.⁸ The higher coercivity of the mechanically alloyed samples may be arising either from the internal strain developed during the process or the absence of grain boundary amorphous phase. To clarify, the samples were annealed in H₂ atmosphere at 300, 400, and 550°C for 1 h and the magnetic properties

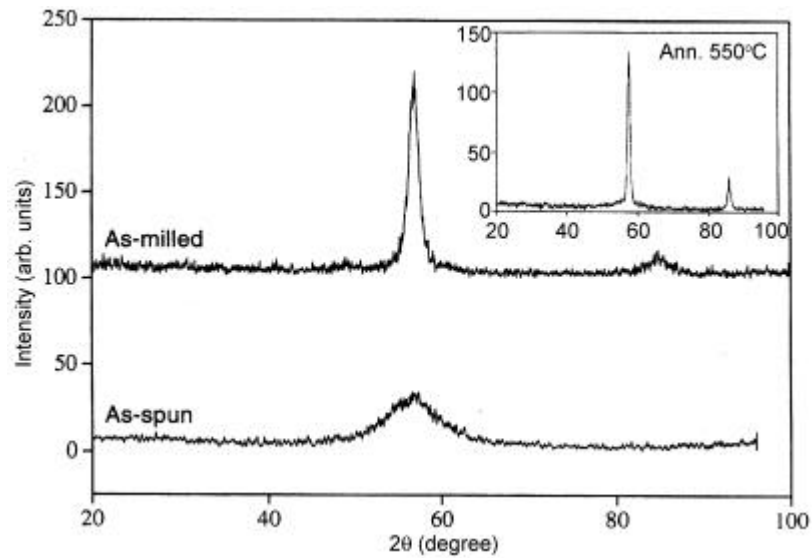


Figure 10. Typical XRD patterns of finemet alloys produced by mechanical alloying (milled for 60 h), melt spinning as well as annealed melt spun ribbon.

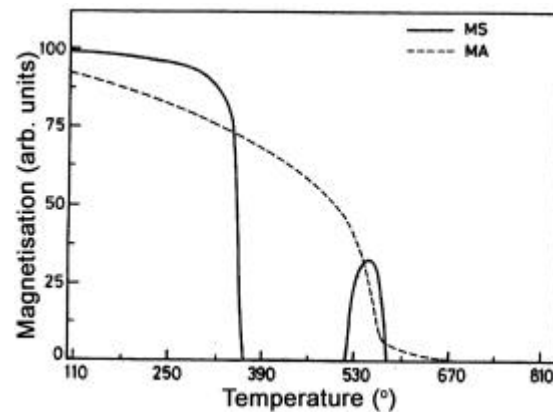


Figure 11. The thermomagnetic curves of mechanically alloyed and melt-spun finemet alloys.

were measured. The strain analysis before and after heat treatment proved that there is significant reduction in the strain level after the heat treatment. However, the coercivity of the samples was found to increase. This indicates that the presence of the amorphous phase enhances the ferromagnetic exchange interaction between α -FeSi nanograins in the suitably annealed melt spun ribbon whereas the absence of amorphous phase weakens the interaction in the mechanically alloyed sample. Hence the magnetic softness of the mechanically alloyed samples is inferior to that of processed melt spun ribbons.

4.2 Magnetic hardening in $\text{Nd}_2\text{Fe}_{14}\text{B}$

$\text{Nd}_2\text{Fe}_{14}\text{B}$ is one of the hard magnetic phases with a wide variety of applications, which also plays a crucial role in the development of exchange spring magnets. The coercivity of the phase decreases when the grain size is smaller than the critical size of single domain due to coupling of the neighbouring grains by exchange interaction. The development of nanocrystalline two-phase magnets (exchange spring magnets), involving $\text{Nd}_2\text{Fe}_{14}\text{B}$ utilizes the high coercivity of the hard magnetic phase together with the easy magnetization of the soft phase. The optimum performance is obtained when the grain size of the hard phase is smaller than the single domain size. Though the coercivity of the exchange spring magnet is lesser than that of the hard phase, it has the potential to be cost effective. The coercivity is also affected by the grain size of the soft phase. The effect of alloying additions in controlling the coercive behaviour of $\text{Nd}_2\text{Fe}_{14}\text{B}$ is studied with 0.1% Cr, Cu and Zr.⁹ Magnetically they correspond to antiferromagnetic, diamagnetic and paramagnetic impurities at room temperature.

Figure 12 shows the X-ray diffraction patterns of the prealloyed, milled and heat treated milled samples. Clearly milling induces amorphisation in the material. Heat treatment for 1-80 kS at 823 K crystallizes the $\text{Nd}_2\text{Fe}_{14}\text{B}$ in the nano-range. The milled samples with additives after heat treatment are identical indicating that the additives do not have any effect on the formation of $\text{Nd}_2\text{Fe}_{14}\text{B}$. The average grain size in these cases

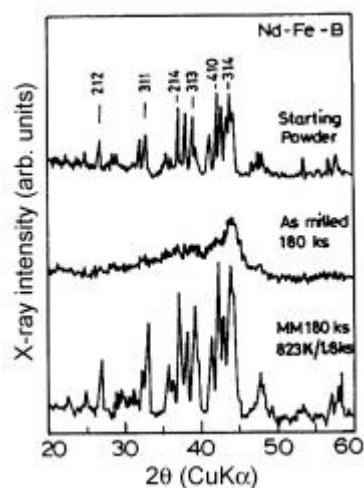


Figure 12. The X-ray diffraction patterns of the prealloyed, milled and heat-treated milled samples of $\text{Nd}_2\text{Fe}_{14}\text{B}$ in the nano range.

was found to be 22 nm. The influence of the small amount of additives on the coercivity in nanograined single domain $\text{Nd}_2\text{Fe}_{14}\text{B}$ materials prepared by mechanical alloying is also studied. Figure 13 shows the variation in coercivity as a function of the applied field for the four samples. Both Cu and Cr addition enhances the coercivity while Zr addition decreases the coercivity. The study concludes with further evidence that the mechanism of magnetic hardening in nanocrystalline $\text{Nd}_2\text{Fe}_{14}\text{B}$ is mostly pinning type proving the importance of the location of impurities in deciding the hardening mechanism.

4.3 Thermoelectric properties of Cu–Te alloys

Tellurides are attractive materials for thermoelectric applications due to their very high thermopower values and ability to yield both *p* and *n* type materials by doping. An improvement of the efficiency of these materials for thermoelectric applications is possible by microstructural control involving grain size reduction. Since a major part of thermal conductivity is controlled by phonon conduction, introduction of a large amount of grain boundaries can lead to scattering and significant decrease in the conductivity. Thus mechanical alloying becomes a potential choice for synthesizing thermoelectric materials. We have investigated the effect of milling on synthesis of Cu_2Te as well as the thermoelectric properties.¹⁵

XRD patterns (figure 14) show that after 6 h of milling, Cu_2Te becomes the prominent phase. Although there exists a large number of phases near the Cu_2Te composition, the observed lines are best fitted with a phase corresponding to hexagonal structure *P6/mmm* with $a = 0.8328$ nm and $c = 0.7319$ nm. The average grain size reduced quickly in the initial hours and stabilized at 10 nm after 40 h. Samples obtained from grinding of prealloyed samples through melting are not significantly different.

The thermopower of the as-cast sample was found to be $37.4 \mu\text{V/K}$, much higher than the reported value for Cu_2Te .²⁷ The discrepancy may be due to the existence of several crystal structures for Cu_2Te . Figure 15 shows the thermo power against milling time for two different compaction pressures. Clearly the thermopower of the mechanically alloyed samples approached the bulk value with long milling times. Higher consolidation pressure showed a quick increase in thermopower within 10–22.5 h while

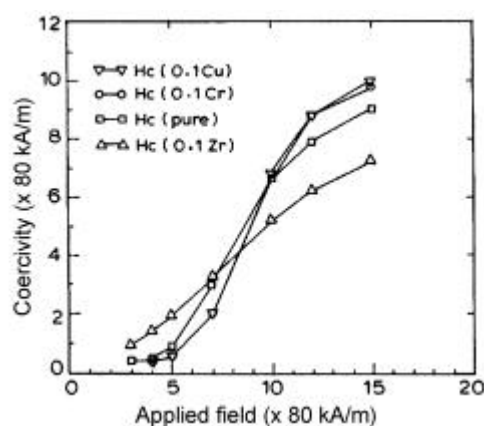


Figure 13. The variation in coercivity as a function of the applied field for the four samples.

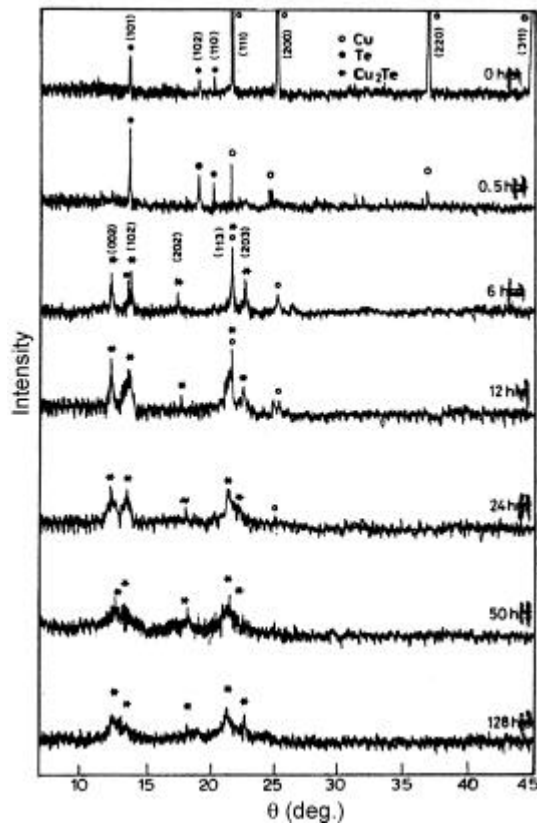


Figure 14. The X-ray diffraction patterns of Cu–Te system as a function of milling time.

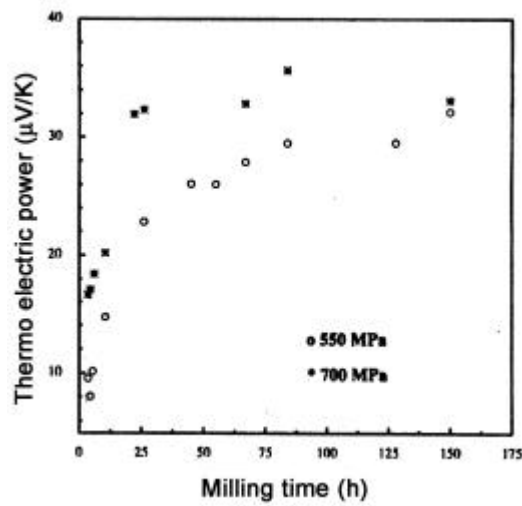


Figure 15. The variation in thermopower against milling time for two different compaction pressures.

the Cu₂Te was forming. However, the melted and ground samples also shows a gradual increase to bulk value indicating the importance of longer milling time.

5. Concluding remarks

The examples cited above clearly point to the usefulness of studying the effects of mechanical energy on simple systems. Such studies enrich our understanding about the process and properties of the resultant products. An increasing understanding of these may allow us to explore new possibilities for mechanical alloying and the mechano-chemical reactions.

Acknowledgements

The authors acknowledge the contribution of their coworkers, Drs M Manivel Raja, K Raviprasad, Chitralekha Jacob, Bhaskar Majumdar, Joyita De, K Sreedhar and Mainak Biswas for some of the work mentioned in this article. Financial support from the Department of Science and Technology, Govt. of India and Council of Scientific and Industrial Research, New Delhi is gratefully acknowledged.

References

1. Benjamin J S 1976 *Sci. Am.* **234** 40
2. Murthy B S and Ranganathan S 1998 *Int. Mater. Rev.* **43** 101
3. Suryanarayana C 2001 *Progr. Mater. Sci.* **46** 1
4. Ding J, Tsuzuki T and McCormick P G 1996 *J. Am. Ceram. Soc.* **79** 2956
5. Schaffer G B and McCormick P G 1989 *J. Appl. Phys. Lett.* **55** 45
6. Takacs L 2002 *Progr. Mat. Sci.* **46** 355
7. Takacs L 2000 *J. Mater. Miner. Met.* **52** 12
8. Manivel Raja M, Chattopadhyay K, Majumdar B and Narayanasamy A 2000 *J. Alloys Compounds* **297** 199
9. Raviprasad K, Ravishankar N, Chattopadhyay K and Umemoto M 1998 *J. Appl. Phys.* **83** 916
10. Chitralekha J, Raviprasad K, Gopal E S R and Chattopadhyay K 1995 *J. Mater. Res.* **10** 1897
11. Majumdar B, Manivel Raja M, Narayanasamy A and Chattopadhyay K 1997 *J. Alloys Compounds* **248** 192
12. Ravishankar N, Abinandanan T A and Chattopadhyay K 2001 *Mater. Sci. Eng.* **A304–306** 413
13. Varghese V, Sharma A and Chattopadhyay K 2001 *Mater. Sci. Eng.* **A304–306** 434
14. Biswas M, Varghese V and Chattopadhyay K 2002 (unpublished work)
15. Sridhar K and Chattopadhyay K 1998 *J. Alloys Compounds* **264** 293
16. Luo H L and Klement W J 1962 *J. Chem. Phys.* **36** 1870
17. Parthasarathy G and Holzapfel W B 1988 *Phys. Rev.* **B37** 8499
18. Tian H H and Atzmon M 1999 *Acta Mater.* **47** 1255
19. Koch C C 1995 *Mater. Trans. Jpn. Inst. Met.* **36** 85
20. Majumder B 1996 *Thermodynamics and microstructural development in immiscible systems processed through different routes*, Ph D thesis, Indian Institute of Science, Bangalore
21. Martin G and Bellon P 1997 *Solid State Phys.* **50** 189
22. Uenishi K, Kobayashi K F, Ishihara K N and Shingu P H 1991 *Mater. Sci. Eng.* **A134** 1342
23. Herr U and Samwer K 1994 In *Solid state phase transformations* (eds) W C Johnson, J W Howe, D E Laughlin and W A Soffa (Warrendale: TMS) p. 1039
24. Baur W H and Rolin J L 1972 *Acta Crystallogr.* **B28** 1448
25. Ferguson G and Trotter J (eds) 1988 *Structure reports* (Metals and Inorganic Sections), International Union of Crystallography (Dordrecht: Kluwer Academic Publishers) vol 55A
26. Alben R, Becker J J and Chi M C 1996 *J. Appl. Phys.* **80** 5209
27. Okhotin A S and Pushkarasky A S 1976 In *Proc. Int. Conf. on Thermoelectric Energy Conversion* (ed.) K R Rao (New York: IEEE)